AN EXPERIMENTAL STUDY ON THE INFLUENCE OF PASSIVE DEFORMATION TO LIFT AND THRUST GENERATION IN FLEXIBLE FLAPPING WING

Fu Peng, Song Bifeng, Wang Liguang
School of Aeronautics, Northwestern Polytechnical University, Xi'an, P.R. China, 710072

Abstract

The influence of deformation on aerodynamic characteristics is studied in this paper. To study the influences of deformation magnitude and range separately, a kind of two-part flapping wing model is designed, which separates the deformation magnitude and range, and makes the measurement of deformation easier. A series of wind-tunnel experiments are carried out to explore the influence. The experimental data shows that deformation has a certain effect on both lift and thrust generation, especially for thrust. The big difference is that the effect on thrust generation is positive, but on lift generation is negative. The wing with smaller deformation range gets more sensitive to deformation magnitude than the wing with larger deformation in thrust generation. This indicates the deformation of the part close to wing tip contributes more to thrust generation than other parts. The result indicates that a proper deformation, including deformation range and magnitude, is helpful to thrust generation but has to have a loss of lift generation.

1 Introduction

Flapping-wing MAV (Micro Air Vehicle) can obtain lift and thrust synchronously from the periodic flapping motions of the flapping wing, which makes the vehicle avoid crashing to the ground and keep forward. So flapping wing is a pivotal part of the vehicle. Inspired by birds, people found a flexible flapping wing had a better performance than a rigid one. Many researches have explored the relationship between aerodynamic force and deformation. Yang W. Q. [1] and Chen L. L. [2] using CFD, considering fluid-structure coupling, studied the influence of structure deformation on aerodynamics, based on N-S equations. In the experimental aspect, Pin Wu, Peter Ifju etc. explored aerodynamics of flexible flapping wing by a lot of experiments [3-5]. All these studies have suggested that appropriate passive deformation produced a positive effect on aerodynamic characteristics of flapping wing.

In general, the flapping wing deformation contains two aspects. One is deformation range, and the other is deformation magnitude. Commonly, a flapping-wing is an indiscerptible unit itself. Different aerodynamic loads may result in different deformation ranges and magnitudes. This makes the deformation range and magnitude hard to be separated and controlled. In order to investigate the influence on aerodynamic characteristics exerted by deformation range and magnitude separately, an experiment was designed and conducted. In this experiment, it's not a complex DIC (Digital Image Correlation) system but a simple angular transducer was used to measurement the deformation, which makes the test easier to be done. In this way, the deformation signal and force signal can be both obtained synchronously. By analyzing the two kinds of signals, something useful can be got.

2 Experiment Method and Models

As stated above, almost all flapping wings have appeared are flexible, and work as a whole. When the wing keeps flapping, the outer part, which has a higher velocity, deforms lager; and the inner part with a lower velocity deforms smaller. So come the two deformation parameters, range and magnitude. These two deformation parameters affect the aerodynamic forces simultaneously. As the flapping or external parameters change, the deformation range and magnitude change synchronously. No way could we have to control them separately to analyze their influences. And for flexible flapping wing, the deformation is hard to be measured. A set of DIC system is required to complete this task, which make it complex to operate.

Considering these contexts, a wind-tunnel experiment is carried out, in which a kind of particular experimental model is designed. To avoid the problems and inconvenience brought by flexible wing, a rigid flapping wing is chosen to simulate the flexible wing. The structure of the experimental model is shown in Fig.1.
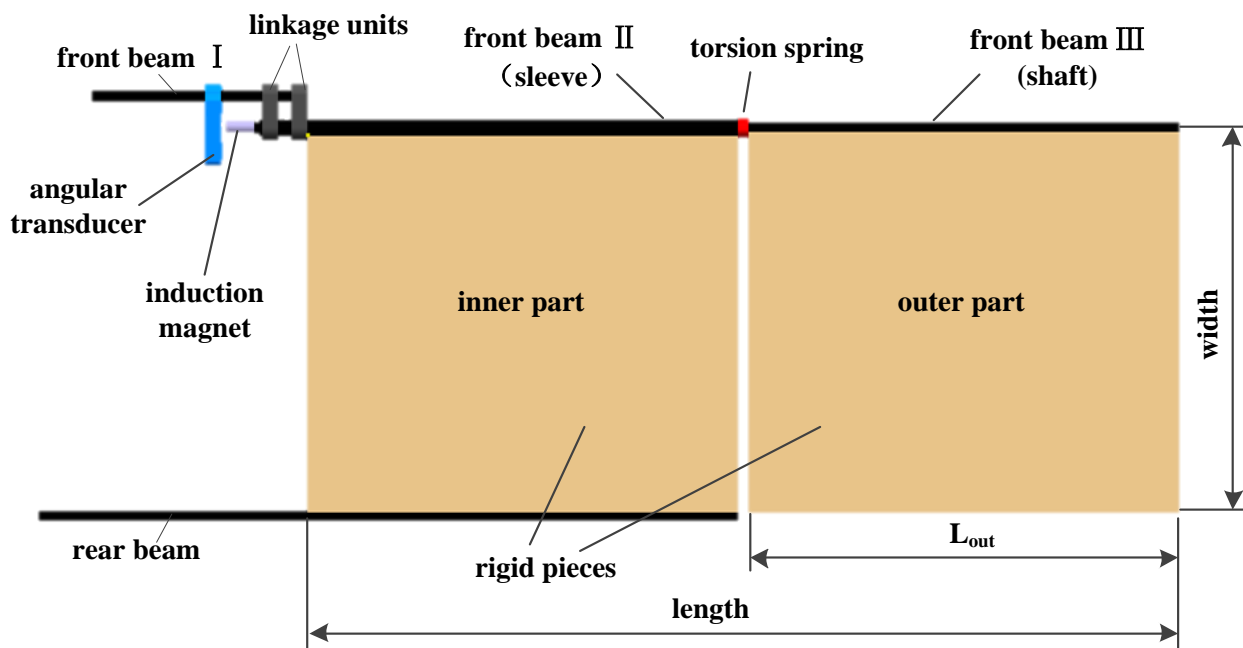

Fig. 1 Structure of the Experimental Model

From Fig. 1, we can see the model is consisted with two parts, the inner part and the outer part, in totally. The two parts are both rigid quadrate pieces made of Balsa Wood. The inner part is fixed on the front beam Ⅱ and rear beam in its leading edge and trailing edge respectively. The front beam Ⅱ is secured to the front beam Ⅰ through two linkage units, and the front beam Ⅰ and rear beam are connected to flapping machine. That is to say, the inner part will perform just like a rigid flapping wing. The outer part is fixed on the front beam Ⅲ. Among the four beams, only the front beam Ⅱ is made of carbon tube, and the other three beams are made of carbon rod. Under the proper sizes, the front beam Ⅲ can pass through the front beam Ⅱ, and rotate around the beam Ⅱ freely. In the other words, the front beam Ⅱ and Ⅲ play the role of sleeve and shaft respectively. The front beam Ⅲ is long enough to reverse a short section out of the front beam Ⅱ at the left end, So that a cylindrical small induction magnet can be installed at that end. When the outer part rotates around the front beam Ⅲ, the induction magnet rotates following the outer part, which transmits the rotation signal into magnetic signal. Based on the hall effect between electricity and magnetism, the angular transducer installed on the front beam Ⅰ transduces the magnetic signal into electrical signal. In that way, the rotation signal can be obtained by measuring the electrical signal. To limit the free rotation, a torsion spring is installed between the front beam Ⅱ and Ⅲ. So

the rotation angle can be controlled by controlling torsional stiffness of the torsion spring. Under the same loads, the lager the torsional stiffness is, the smaller the rotation angle will be.

In the flapping motions, the out part will have a rigid rotation relative to the inner part under the action of aerodynamic loads. The inner part and outer part are used to play the roles of undeformed part (or small deformed part) and deformed part of flexible flapping wing. L_{out} (length of the out part) is used to simulate the deformation range, and the rotation angle is used to simulate the deformation magnitude.

In order to explore the aerodynamic characteristics of flexible flapping wing in different deformation ranges and magnitudes, a series of experimental models are designed and made. These models have the same shape and size. Their lengths are 160mm, and widths are 70mm. The differences are the different out part sizes (L_{out}) and the different torsion springs with different torsional stiffness. To control the deformation magnitude (rotation angle), five different kinds of torsion springs are chosen. To control the deformation range, five different value of L_{out} are arranged. The values of L_{out} are 40mm, 60mm, 80mm, 100mm and 120mm. The percentages of deformation range relative to the wings are 25%, 37.5%, 50%, 67.5% and 75%. So a total of 25 models are included. These models are arranged into five sets according to L_{out}. Each sets contains five models with different torsion springs. Fig. 2 shows the photos of five models with different L_{out}.

L_{out}=40mm L_{out}=60mm

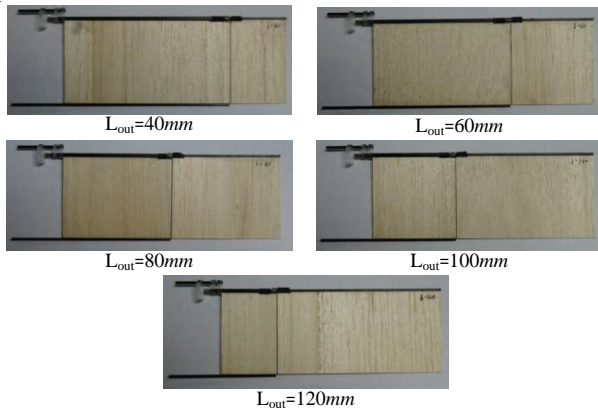L_{out}=80mm L_{out}=100mm

L_{out}=120mm

Fig. 2 Actual Experimental Models

3 Experiment Set Up

This work is conducted in a small wind tunnel facility in Northwestern Polytechnical University. The wind tunnel is built for MAV tests specially. The wind tunnel total length is 6.251m. The test section measures 70cm (Length) $\times$ 50cm (Width) $\times$ 50cm (Height), and has an inlet contraction ratio of 4. The flow speed range in the tunnel is 3～19m/s, with a 0.02% turbulence level.

Fig. 3 The Wind Tunnel Facility

In order to measure the aerodynamic forces, a three-component small capacity balance is used. The measure ranges of this balance are 16N in lift direction, 8N in drag direction and 0.7$N\,m$ in pitching moment direction. The measurement uncertainty (95% confidence level) is less than 1.00%.

In the test, a flapping machine is designed and made to accomplish the wing's flapping motion, shown in Fig. 4(a). The flapping machine is consisted of driven motor and transmission mechanism. A FAULHABER brushless servo motor is used as the driven motor. The motor can provide extremely accurate control of rotate speed by its closed loop control system. With its CAN bus communication, the voltage signal, current signal and position signal in operating can be feedback in real time. With this motor, the maximum flapping frequency is up to 12Hz. A four-bar linkage model is adopted in the design of this flapping machine, which makes the machine simple and practical. Six connecting threaded holes are arranged in the crank flange connected with the output shaft of the motor. By connecting different threaded hole between crank flange and rod, the flapping angle can be set to 31.8°, 42.8°, 54.3°, 66.6°, 80.1° and 96.0°. The 54.3° flapping angle is chosen in this wind tunnel test. The flapping motion is transmitted by the two meshing gears between the two

rockers. This mode keeps the two rods to flap completely symmetrically. The selected parameters of the machine result in a near-sinusoidal kinematics profile output.
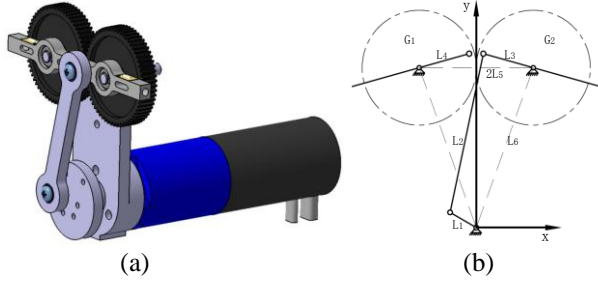

(a)   (b)

Fig.4 The Flapping Machine
(a) The 3-D Model; (b) Schematic Diagram

A set of data acquisition (DAQ) system based on NI CompactDAQ-9188 is applied in the test. Several C-serial DAQ and control boards are used. The force signals are acquired by NI 9215 with a 16-bit resolution, and other analog signals are acquired by NI 9201 with a 12-bit resolution. The driven motor is controlled by NI 9862, whose transmission speed is up to 1Mbit/s. The entire setup is automated by a specially written LabVIEW 2010.

4 Data Analysis

4.1 Removement of Inertial Force

In the flapping motions, inertial force of flapping wing exists all the time. The forces we measured are the mixture of inertial and aerodynamic forces. To obtain the pure aerodynamic force, the inertial force should be removed out

In the test, the inertial force is calculated based on the flapping wing's physical property and motion state. For different motion states, the inertial forces of the inner and outer parts are calculated separately. Here the two parts are regarded as two particles for calculating. The motion of the inner part is simple, just rotating around flapping axis, driven by flapping machine. Besides the same motion as the inner part, the outer part rotates around the leading edge additionally.

The inner part: The motion of the inner part is a pure two-dimension flapping motion.

The dynamics model is shown in Fig. 5. O is the flapping axis; m_{in} is the mass center. z coordinate points the F_z direction of the balance, and y coordinate points the direction of side force. The acceleration can be represented as follows:

$$\begin{cases} a_{n\_in} = \dot{\theta}^2 r_{in} \\ a_{t\_in} = \ddot{\theta} r_{in} \end{cases} \tag{1}$$

Where, a_{n_in} and a_{t_in} are centripetal acceleration and tangential acceleration, θ is flapping angle, and r_{in} is the distance between rotation axis and mass center. If we define $\boldsymbol{i}$, $\boldsymbol{j}$, $\boldsymbol{k}$ as three unit vectors in the direction of x, y, z coordinates, the resultant acceleration $\boldsymbol{a_{in}}$ can be represented as follows:

$$\mathbf{a_{in}} = a_{in\_y}\mathbf{j} + a_{in\_z}\mathbf{k} \tag{2}$$

Where, $\begin{cases} a_{in\_y} = r_{in}(\dot{\theta}^2\cos\theta + \ddot{\theta}\sin\theta) \\ a_{in\_z} = r_{in}(\dot{\theta}^2\sin\theta - \ddot{\theta}\cos\theta) \end{cases}$.

So the inertial force can be represented as follows:

$$\begin{aligned} \mathbf{F_{in}} &= F_{in\_y}\mathbf{j} + F_{in\_z}\mathbf{k} \\ &= -m_{in}(a_{in\_y}\mathbf{j} + a_{in\_z}\mathbf{k}) \end{aligned} \tag{3}$$

Where, m_{in} is the mass of the inner part. F_{in_y} and F_{in_z} are two components of inertial force in the direction of y and z coordinates.
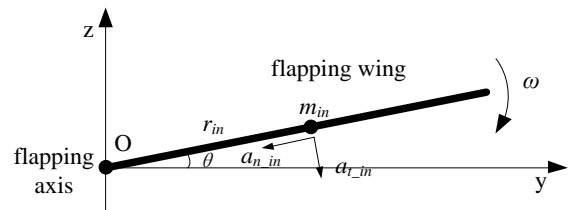

Fig. 5 Dynamics Model of the Inner Part

The outer part: The motion of the outer part is more complex relatively. It is a resultant motion of two rotation motions, seeing in Fig 6. If we regard the flapping motion as carrier motion, and regard the rotation motion around the leading edge as relative motion, the acceleration of the out part can be represented as follows:

$$\mathbf{a_{out}} = \mathbf{a_e} + \mathbf{a_r} + \mathbf{a_k} \tag{4}$$

Where, $\boldsymbol{a_e}$, $\boldsymbol{a_r}$ and $\boldsymbol{a_k}$ are carrier acceleration, relative acceleration and Coriolis acceleration.
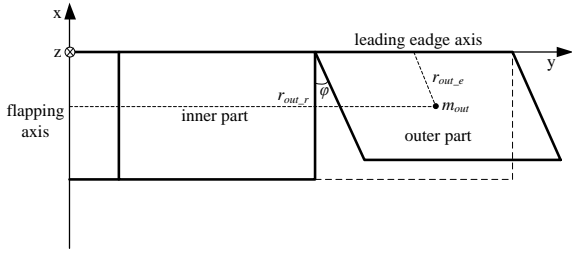
Fig. 6 Motion State of the outer part

Similarly, $\mathbf{a}_e$ and $\mathbf{a}_r$ can be calculated with the following equations:

$$\begin{cases} \mathbf{a}_e = a_{e\_y}\mathbf{j} + a_{e\_z}\mathbf{k} \\ \mathbf{a}_r = a_{r\_x}\mathbf{i} + a_{r\_y}\mathbf{j} + a_{r\_z}\mathbf{k} \end{cases} \quad (5)$$

Where,
$$\begin{cases} a_{e\_y} = r_{out\_e}(\dot{\theta}^2\cos\theta + \ddot{\theta}\sin\theta) \\ a_{e\_z} = r_{out\_e}(\dot{\theta}^2\sin\theta - \ddot{\theta}\cos\theta) \end{cases}$$

and
$$\begin{cases} a_{r\_x} = r_{out\_r}(\dot{\varphi}^2\cos\varphi + \ddot{\varphi}\sin\varphi) \\ a_{r\_y} = r_{out\_r}(\dot{\varphi}^2\sin\varphi - \ddot{\varphi}\cos\varphi)\sin\theta \\ a_{r\_z} = r_{out\_r}(\dot{\varphi}^2\sin\varphi - \ddot{\varphi}\cos\varphi)\cos\theta \end{cases}$$

r_{out_e} and r_{out_r} are the distances from the mass center of the outer part to the flapping axis and leading edge axis; φ is the rotation angle relative to the inner part. According to the two rotation motions, $\mathbf{a}_k$ can be represented as follows:

$$\mathbf{a_k} = -r_{out\_r}\dot{\theta}\dot{\varphi}\cos\varphi\mathbf{j} \quad (6)$$

So the inertial force of the outer part is:

$$\mathbf{F_{out}} = -m_{out}\mathbf{a_{out}} = -m_{out}(\mathbf{a_e} + \mathbf{a_r} + \mathbf{a_k}) \quad (7)$$

Where, m_{out} is the mass of the outer part.

Combining the equation (3) and (7), the inertia force of the flapping wing can be expressed as follows:

$$\mathbf{F_{ine}} = \mathbf{F_{in}} + \mathbf{F_{out}} \quad (8)$$

4.2 Deformation characters

The deformation of the flapping wing is the rotation of the outer part around the leading edge actually. The deformation angle is determined by the stiffness of the torsion spring (inhibition effect) and the external loads exerted on the outer part (promoting effect). When the wing flaps, an alternating deformation angle will occur under the periodic load. Fig. 7 shows the deformation characteristics in two flapping cycles, in which the length of outer part is

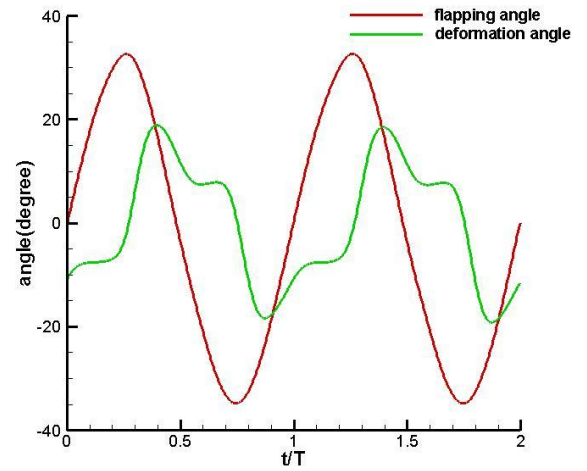80mm, the flapping frequency and air speed are 6Hz and 0m/s.

Fig. 7 Deformation Characteristics of the Outer Part

As seen in Fig. 7, the period character is obvious. A near 90 degree phase difference exists between the two curves. When the wing moves to horizontal position (zero degree of flapping angle) nearly, the largest deformation takes place. When the wing moves to near the highest and lowest positions, the deformations is closed to zero. The appearance of this phenomenon is leaded to by the combination of aerodynamic force and inertial force. Different experimental conditions may cause different phase differences and magnitudes.

4.3 Thrust

The thrust measured in the test is not the pure thrust but the resultant force in the direction of thrust, including pure thrust and drag. In this test, the influence of deformation range and magnitude on thrust and lift generation is intended to be explored.

The thrust changing with deformation can be seen in Fig. 8 and Fig. 9. They show the changing curves of deformation angle (deformation amplitude) and corresponding thrust in a flapping cycle. The five wings (No.1~No.5) are a set of test models with different torsion springs. From No.1 to No.5, the torsional stiffness becomes stronger in turn. The L_{out} of the five wings is 80mm. And the experimental environment is also exactly the

5

same: the air speed, flapping frequency and attack angle are 5*m/s*, 8*Hz* and 0 °respectively.
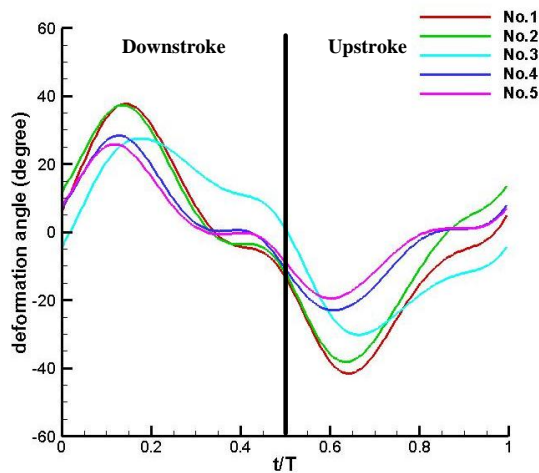

Fig. 8 Deformations of Five Wings with Different Torsion Springs in a Flapping Period
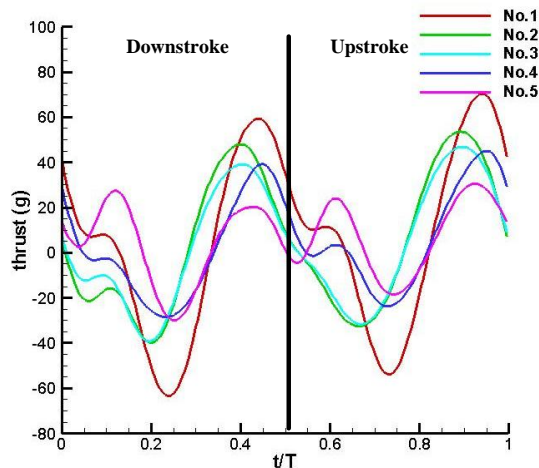

Fig. 9 Thrusts Generation of Five Wings with Different Torsion Springs in a Flapping Period

From Fig.8, we can see the changing tendencies of the five curves are almost the same, but the magnitudes are different. The stronger the torsional stiffness of the wing is, the smaller the deformation magnitude is. In the analysis, the average value of peak and valley is regarded as the deformation magnitude of the wing flapping in the corresponding condition. In Fig.9, the corresponding thrust curves are shown. In a flapping cycle, the thrust have two peaks and two valleys. Different torsional stiffness leads to different magnitude of thrust. Combining with Fig.8, we can find larger

magnitude of deformation results in lager magnitude of thrust. This illustrates that deformation magnitude plays a positive role in thrust generation of flexible flapping wing in the deformation range in the test.

The average thrust is shown in Fig. 10 in the same test condition. The figure contains the average thrusts of five sets of wings in different deformation angles. The cyan curve (L_{out}=80*mm*) is the combination of Fig. 8 and Fig. 9, which shows that not only the magnitude of thrust but also the average thrust is affected positively by deformation magnitude.
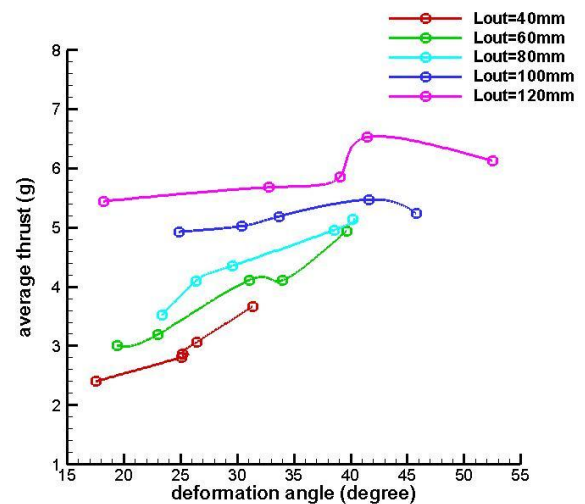

Fig.10 Average Thrusts of Wings with Different L_{out} in Different Deformation Angles

Because of different loads exerted on the outer parts, the wings with different L_{out} have different deformation magnitude. This can be seen from Fig. 10 easily. The wings with L_{out}=120*mm* deform much larger than the wings with L_{out}=40*mm*. From the figure, we can see when deformation angel is less than 42 °, the average thrust grows with deformation angel; but when deformation angle excesses 42 °, the average thrust begins to drop. That is to say, just like the lifting line of fixed wing, there also exists a certain threshold of the deformation angle, the thrust grows with the deformation angle only among the range of threshold, or an opposite phenomenon would occur. In addition, the curve with longer L_{out} locates in a higher position than the curve with shorter L_{out} in Fig. 10, but becomes more gradual. This indicates that in the same condition of deformation angle, the wings with larger deformation ranges

generate larger thrust, but has a lower growth rate relative to deformation angle.

4.4 Lift

Since a flat wing without any airfoils cannot produce any average lifts in symmetric flapping motions, an experimental condition with an attack angle is chosen to be analyzed. Fig. 11 and Fig. 12 are the instantaneous values of deformation angles and lifts of a set of five wings in one stroke cycle. The L_{out} of the models is 120mm. The air speed, flapping frequency and attack angle are 8m/s, 8Hz and 9 °. The five models have five different torsion springs with different torsion stiffness. From No.1 to No.5 the stiffness becomes stronger in turn.

From Fig.11, we can easily find that from No. 1 model to No. 5 model, the deformation angles decrease in turn, commensurate with their different torsion stiffness. Corresponding with their lifts shown in Fig. 12, we find the curves of lifts in one stroke cycle change with deformation angel. The wing with a larger deformation angle has a lower lift. This can also be sustained by the average value of lift. In Fig. 13, the pink curve shows the changing tendency of average lift influenced by deformation angle, combining with Fig. 11 and Fig. 12. The changing tendency indicates the average lift decreases with the increasing of deformation angle. That is to say, deformation has a negative effect on lift generation. This is absolutely contrary to the influence of deformation angle on thrust generation.
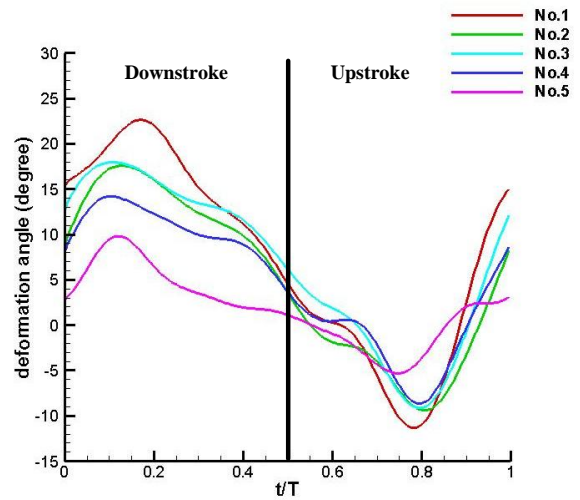

Fig. 11 Deformations of Five Wings with Different Torsion Springs in a Flapping Period
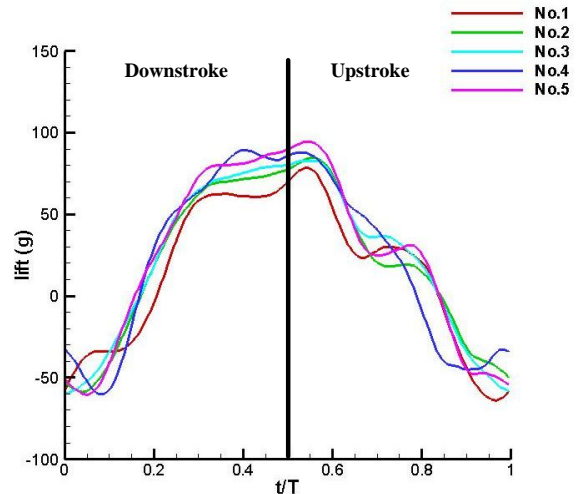

Fig. 12 Lifts Generation of Five Wings with Different Torsion Springs in a Flapping Period

Fig. 13 shows the curves of average lifts of all five sets of wings changing with deformation angles. On the whole, the changing tendencies of the five curves with different L_{out} are basically consistent. The downward trend indicates deformation is not conducive to lift generation, and the larger the deformation angle is, the more unfavorable the effect on lift generation is. Under the same condition of deformation angle, the wings with longer L_{out} have smaller lifts generated. In other words, deformation, no matter range and magnitude, plays a negative role in life generation, and the increasing of deformation intensifies this effect.
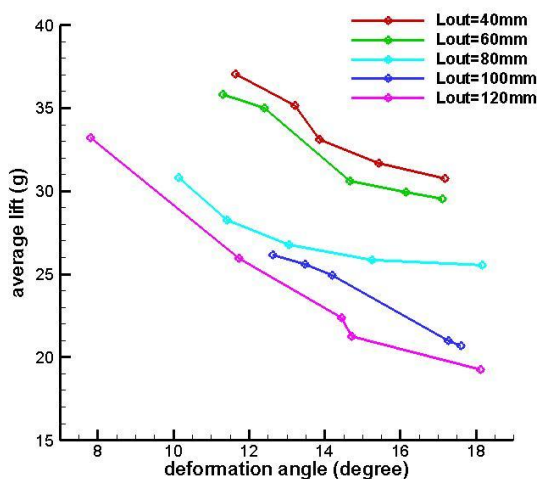
Fig.13 Average Thrusts of Wings with Different L_{out} in Different Deformation Angles

5 Result

Rigid flapping wing produces almost no effective average thrust in a stroke cycle. So the flexible flapping wing is adopted by almost all flapping MAVs. The passive deformation of flapping wing effectively improves the performance in flapping flight.

The experimental result shows that the deformation of flapping wing has significant effect on the aerodynamic characteristic. The deformation magnitude can increase the oscillating range and average thrust at the same time, but too large deformation magnitude is harmful to thrust generation. When the deformation magnitude is larger than 43°, the average thrust begins to fall. The deformation range seems always helpful to thrust generation. The average thrust increases as the enlargement of deformation range. But wing with larger deformation range has a lower growth rate with deformation magnitude. This means the deformation part close to the wing tip is more efficient in thrust generation.

Oppositely, the deformation is not conducive to lift generation. The enlargement of deformation magnitude and range leads to the decrease of the oscillating range of lift and average lift.

So, the contradictory phenomena determine that we cannot keep the good points of lift and thrust both. From Fig.10 and Fig. 13, we can summary that a flapping wing with larger deformation range and smaller deformation magnitude is more reasonable. When designing a flexible flapping wing, we should arrange the stiffness distribution reasonably to make the outer part have a larger deformation magnitude, and make the other part have a smaller deformation magnitude. which can satisfy the requirements of lift and thrust both.

References

[1] Yang WenQing, Song BiFeng, Song WenPing and Li ZhanKe. Fluid-structure Coupling Research for Micro Flapping-Wing. *27th International Congress of the Aeronautical Sciences*, 2010.

[2] Chen L L, Song B F, Song W P, et al. Research on aerodynamic-structural coupling of flexible flapping wings. *Acta Aeronautica et Astronautica Sinica*, 2013, 34(12): 2668-2681.

[3] Erik Sallstrom, Lawrence Ukeiley, Pin Wu and Peter Ifju. Aerodynamic Forces on Flexible Flapping Wings. *49th AIAA Aerospace Sciences Meeting including the New Horizons Forum and Aerospace Exposition*, 4-7 January 2011. AIAA 2011-569.

[4] Pin Wu, Peter Ifju and Bret Stanford. Flapping Wing Structural Deformation and Thrust Correlation Study with Flexible Membrane Wings. *AIAA JOURNAL*, Vol. 48, No. 9, September 2010.

[5] Wu P., Stanford B., and Ifju, P. Passive bending and twisting motion during the flapping stroke of a micro elastic wing for thrust production. *AIAA Aerospace Sciences Meeting and Including the New Horizons Forum and Aerospace Exposition*, January 2009. AIAA 2009-879.

Contact Author Email Address

mailto: fupeng0416@163.com